NASA-TM-112140

AIAA 95-6011
Airbreathing/Rocket Single-Stage-to-Orbit Design Matrix

James L. Hunt
NASA Langley Research Center
Hampton, Virginia

Sixth International Aerospace Planes and Hypersonics Technologies Conference
April 3-7, 1995/Chattanooga, TN

AIRBREATHING/ROCKET SINGLE-STAGE-TO-ORBIT DESIGN MATRIX

by
James L. Hunt
NASA Langley Research Center
Hampton, Virginia

ABSTRACT

A definitive design/performance study was performed on a single-stage-to-orbit (SSTO) airbreathing propelled orbital vehicle with rocket propulsion augmentation in the Access to Space activities (Ref. 1 and 2; Option III Team) during 1993. A credible reference design was established, but by no means an optimum. The results supported the viability of SSTO airbreathing/rocket vehicles for operational scenarios and indicated compelling reasons to continue to explore the design matrix. This paper will (1) summarize the Access to Space design activity from the SSTO airbreathing/rocket perspective, (2) present an airbreathing/rocket SSTO design matrix established for continued optimization of the design space, and (3) focus on the compelling reasons for airbreathing vehicles in Access to Space scenarios.

INTRODUCTION

Airbreathing/rocket powered, single-stage-to-orbit, horizontal takeoff and landing (HTOL) aerospace planes are highly integrated systems with unprecedented levels of interdisciplinary interactions involving a broad spectrum of technologies. The level of coupling between propulsion systems, propellant systems, auxiliary power systems, control systems, thermal management systems, and airframe, and especially the couplings between the propulsion flowfield and the aerodynamic flowfield require that these vehicles be more intensely integrated than has ever been attempted. While this high level of systems and discipline integration complicates the design process, as it does to a lesser extent for high performance airplanes, it is the key to greater performance potential—ground/flight operations flexibility, launch/flight safety and reliability, and larger payload fractions to orbit.

An airbreathing/rocket single-stage-to-orbit (A/R SSTO) vehicle design is rich in variables and can evolve to a robust flexible machine through a highly optimized design process if the systems/disciplines are integrated synergistically and the appropriate technologies matured. Such a robust A/R SSTO vehicle can provide routine access to orbit, not only at a substantial cost reduction, but with tremendously increased operational flexibility (ground and flight) and reliability. Many of these attributes stem from the airplane characteristics of this vehicle, such as lifting body, airbreathing propulsion, horizontal takeoff and landing, ferry and cruise capability, etc. The A/R SSTO is an airplane that flies to orbit and as such it can be expected to accrue many of the desirable operational characteristics associated with contemporary high performance aircraft. Specifically, they materialize through:

- Gradual step and check engine start-up and shutdown
- Horizontal takeoff/abort capability
- In atmospheric abort during ascent with powered flyback
- Relatively low noise levels
- Large launch window potential
- Launch offset capability
- Orbital plane change through in-atmosphere lifting/powered maneuvers
- Large cross range capability
- Subsonic and/or supersonic ferry capability
- Hypersonic cruise capability

In addition to providing the basis for major improvements in future launch vehicles, the technologies developed for A/R SSTO vehicles will also enable the development of high speed aircraft for both civil and military needs. These hypersonic aircraft (M>8) can also serve as first stages of orbital access systems for small orbital payloads as long as the upperstage is encloseable in the aircraft payload bay. This staging capability would require a rocket in the tail end of the aircraft to perform a pull-up maneuver to reach low dynamic pressures for staging. Of course, an airbreathing SSTO can also serve as a hypersonic airplane. Thus, there is tremendous synergy, not only in the technologies of these vehicles, but in the configuration and the utility...both space access and endoatmospheric.

The airbreathing propulsion system for the airbreathing/rocket powered vehicle presented herein (Figure 1) consists of a low-speed system and a ramjet/scramjet that are housed in an engine nacelle underslung to the midsection of a lifting-body fuselage. The forebody undersurface of the vehicle acts as an external inlet, precompressing air for delivery to the inlet/combustor and the aftbody undersurface acts as an external nozzle for the expansion of exhaust gases. This results in an airbreathing propulsion system that is totally integrated from nose to tail on the underside of the vehicle. Changes in throttle setting change the forces in the nozzle, and in turn, require a change in aerodynamic controls and vehicle attitude to maintain stable flight. Above Mach 15, LOX augmentation of the scramjet is used to increase thrust margin as the vehicle begins to pull up from its high dynamic pressure trajectory; thus, the airbreathing propulsion flowpath transitions to a hybrid system with some of the characteristics of a rocket.

An independent modular rocket system configured with a linear aero-spike nozzle is integrated in the trailing edge of the fuselage. It provides thrust augmentation during takeoff, transonic acceleration, and acceleration above Mach 15; it is used for orbital insertion and, in space, as an orbital maneuvering system (OMS) in conjunction with the separate reaction control system (RCS).

Another important coupling involves thermal management. Since the vehicle accelerates to low Earth orbit through an airbreathing corridor at high dynamic pressures, the heat load during ascent is approximately twice that which occurs during reentry and descent. During descent, the heat load is less because of low planform loading and low angle-of attack. In order to manage this ascent heat load, the cryogenic hydrogen fuel is used to actively cool the engines, portions of the forebody inlet ramp and the nozzle expansion surface, and the leading edges of the airframe. In this manner, the use of heavy, very high-temperature materials is minimized. Also, the more heat absorbed by the fuel, the more power that can be extracted from the fuel system network to drive pumps, etc. and/or the higher the fuel injection temperature—a factor that enhances propulsion efficiency and vehicle performance.

The high degree of systems integration and performance coupling provides "forgiving" vehicle characteristics. If, for example, the propulsion system does not attain the maximum efficiency predicted, the trajectory and the trajectory events can be re-optimized by increasing the use of liquid oxygen (LOX) augmentation. This can be done in both the airbreathing scramjets and the external rockets (when they are initiated in the high Mach number portion of the trajectory) to increase the thrust-to-drag ratio of the vehicle, and thus, compensate for scramjet propulsion efficiency losses, should they occur.

VEHICLE DESCRIPTION/ CLOSURE OVERVIEW

In support of NASA's Access to Space Study (Ref. 1 and 2), a viable baseline A/R SSTO vehicle design with a 15% weight growth margin was developed by the Langley Research Center's Systems Analysis Office. The vehicle was designed to carry 25,000 lbs. of payload in a 15'x15'x30' rectangular payload bay to an orbit of 220 nm, 51.6° inclination, then dock with a hypothetical space station for delivery of the payload (Ref. 1 and 2). The A/R SSTO vehicle has a 5-minute launch window and an ascent delta velocity margin of 1%. The baseline design, as shown in Figure 1, consists of:

- A wedge-shaped forebody profile, spatula-shaped forebody planform, lifting-body configuration with all moving horizontal tails, twin vertical tails with rudders, and trailing edge body flaps.

- Underslung, 2-D airbreathing engine nacelle for which the vehicle forebody serves as a precompression surface and the aftbody as a high expansion ratio nozzle; two engine systems with 130K lbs. of thrust each at takeoff.

- Linear modular, aerospike rocket engine at the trailing edge; two engine systems with 117K lbs. of thrust each at takeoff.

- Slush hydrogen fuel (SH2) and Liquid Oxygen oxidizer (LOX) propellant (about a 50/50 split by weight).

- Actively cooled leading edges (fuselage spatula-shaped region and engine cowl); actively cooled, non-integral panels in engine.

- A 15'x15'x30' rectangular payload bay located in the vehicle mid-section with two "shuttle-like" doors that swing to the (top) of the vehicle.

- A crew station adjacent to the payload bay with access/escape from the vehicle topside and conduit to the payload bay.

- Two 6-wheel main landing gears; one nose gear (two wheels).

- Baseline vehicle airframe structure/tank/ thermal protection system (TPS)

    - Graphite/epoxy (Gr/Ep) integral, I-stiffened, conformal slush hydrogen (SH2) tank
    - Aluminum/Lithium (Al/Li) non-integral, multilobe liquid oxygen (LOX) tanks
    - Gr/Ep shell structure fore and aft of integral tank; Titanium Matrix Composites ((TMC), Silicon carbide/beta 21s titanium) all moving horizontal controls and twin verticals/rudder with Carbon/Silicon carbide (C/SiC) TPS over portions exceeding 1960°R; carbon-carbon (C/C) leading and trailing edges
    - Fibrous Refractory Composite Insulation (FRCI-12) over Rohacell insulation on windward surface and Tailorable Advanced Blanket Insulation (TABI) over Rohacell insulation on leeward surface.

The airbreathing corridor to Mach 25 and the engine mode changes experienced in this acceleration process also characterize this aerospace plane. A representative ascent trajectory for the A/R SSTO vehicle is presented in Figure 2 including indicators for propulsion mode events. Most of the airbreathing propelled ascent is along a high dynamic pressure isobar (2150 psf). Takeoff and transonic ascension are accomplished with the low-speed system and external rocket system performing simultaneously. The rocket is switched off at about Mach 1.8; the ramjet mode is initiated at Mach 3. Transition to the scramjet begins at Mach 6 with the full scramjet mode in operation by Mach 7.5. Departure from the isobar above Mach 15 signals the onset of LOX augmentation through the scramjet and the activation of the external rocket system as indicated in Figure 2. Scramjet main engine cutoff (MECO) is at Mach 24. Even though the external rocket system has essentially the same thrust at takeoff as the airbreathing engines, the airbreathing flowpath provides 83% of the total ascent energy.

The baseline A/R SSTO vehicle closure weights for the previously described mission are presented in Figure 3. The takeoff gross weight (TOGW) is 702,000 lbs.; the dry weight (DW) is 176,000 lbs. Adding a 15% dry weight growth margin, as specified in the Access to Space Study, increased the TOGW to 917,000 lbs. and the DW to 239,000 lbs. (Ref. 1 and 2). The length of the closed vehicle with 15% dry weight growth is 200 ft.

Configuration Characteristics

The spatulated lifting-body configuration was selected because it has:

- large air delivery to the inlet system and low aerodynamic drag per unit maximum-cross-section of the fuselage...high capture

per unit drag resulting in high thrust-to-drag ratios.
- 2D-like forebody flow with little crossflow and inlet distortion
- low planform loading
- high lift curve slope

The configuration geometric characteristics are:
- fineness ratio = 5.7
- planform power law = 0.2

It should be noted that this configuration is not optimized; much work remains in refining the characteristics to provide an optimum shape for the mission in this configuration space, let alone the work required in examining/resolving higher fineness ratio wing body configurations.

PROPULSION

Airbreathing Systems

The airbreathing propulsion flowpath consists of the lower surface of the vehicle from the apex of the spatula-shaped leading edge to the end of the aftbody nozzle at the trailing edge of the vehicle. The flowpath is further defined by those surfaces wetted by flow that passes through the engine nacelle underslung to the midsection of the lifting-body fuselage. The airbreathing engine systems, however, are confined to the nacelle and the volume just above the nacelle.

The A/R SSTO vehicle propulsion system design consists of two engine systems. The engine flowpaths were sized to accommodate the width of the baseline A/R SSTO vehicle fuselage design.

The airbreathing engine system integrated into a single duct nacelle. It consists of:

- A low-speed system that operates from Mach 0 to 3.
- A dual-mode ramjet that operates from Mach 3 to 5. The duct between the rearward combustor and the forward throat forms the isolator that maintains the head pressure against which the ramjet combustor operates.
- A ramjet to scramjet transition that occurs from Mach 6 to 7.5. During this transition, the fuel injection is being moved forward in the combustor.

- A scramjet that operates from Mach 8 to 15. The fuel is injected essentially parallel to the flow.

- A LOX augmented scramjet that operates from Mach 15 to MECO at Mach 24.

The cycle code, SRGULL (Ref. 3), was used to predict the airbreathing flowpath (ramjet/scramjet) performance for the A/R SSTO vehicle.

External Rocket System

The A/R SSTO vehicle is equipped with an augmented expander-cycle linear- rocket system designed to provide (1) primary thrust for orbit insertion and deorbit and (2) auxiliary thrust for take-off, transonic push-through, high Mach number acceleration and mission abort. When used in an auxiliary mode with the low speed propulsion system for take-off, the external rocket system (ERS) reduces vehicle take-off speed and distance. The platelet thrust cell technology for this ERS has been developed by Aerojet and McDonnell Douglas under the government sponsored Linear Rocket Technology Program (Ref. 4).

The thrust level of the ERS for the baseline A/R SSTO is 234K lbs. at sea-level. The system is installed in the aft end of the vehicle (Figure 1); it is blended with the vehicle mold line to provide low drag and minimal impact on main engine performance.

The ERS is configured with eight rocket modules (four top, four bottom) that are arrayed across the aft portion of the vehicle (Figure 4); the 2-D expansion nozzle is integrated into the rear of the fuselage. Vehicle pitch, roll and yaw control can be achieved by differentially throttling or selectively firing appropriate rocket modules; however, the aerodynamic surface controls are relied on solely for that purpose during ascent for this A/R SSTO vehicle design. Each module consists of six 2-D platelet chambers.

The rocket system is a dual, augmented expander-cycle linear rocket which operates with a low turbine inlet temperature and provides a 10:1 throttling capability. High sea-level, static efficiency is a favorable characteristic of linear rocket systems since the nozzle flow does not separate at high back pressures, as it does in bell nozzles. All turbomachinery for the ERS is separate from the main engine system.

STRUCTURES

Airframe Structure

Description of Structural Design:

For the A/R SSTO baseline vehicle design, a cold integral-tank concept with a bonded-on thermal protection system (TPS) was selected. This design was chosen for a combination of reasons including attractive structural weight, volume, and cost.

The general structural arrangement of the A/R SSTO baseline vehicle with the cold, integral tank architecture is shown in Figure 5. The cold integral tank concept uses the same basic structure both to contain the pressurized fuel and to carry airframe flight loads. The shape of the structure is maintained under pressure through the use of cross-sectional shape control members which are spaced at 36 inches over the length of the vehicle. These members are constructed of a membrane sheet which has cut-outs to allow fuel movement, as shown in Figure 6. They are stabilized with vertical stiffeners between upper and lower surfaces of the tank shell. The stiffeners are constructed of hat-sections applied back-to-back on the membrane, as shown in Figure 7. Attachment to the tank shell is accomplished with bonded clips on the longitudinal skin stiffeners. This arrangement allows the free flow of fluids or gas along the interior of the tank shell, thus preventing the entrapment of excess ullage and allowing liquid to freely drain to suction pumps.

In addition to the shape control members, longitudinal, vertical shear webs are provided at four places across the vehicle as shown in Figure 6. These webs carry vehicle shear, induced by flight maneuver loads and act to stabilize the fuselage shell against buckling. The shear webs and shape control members also act to stabilize the individual shell panels against panel buckling. Tank pressure is contained by the stiffened shell with resulting loads transmitted to the shape control members and shear webs. In addition, the longitudinally stiffened skin provides the primary bending stiffness required to carry the vehicle flight loads. At locations of substantial load in the fuselage, additional bulkheads are required. These are at slope changes in the shell surface, LOX tank attachments, landing gear locations, wing carry-through and engine truss attachments. The basic tank shell structure extends to the front and rear of the hydrogen carrying sections to form the complete load carrying airframe and house the non-integral, aluminum-lithium liquid oxygen (LOX) tanks. In these areas, the shell structure is not internally pressurized.

The main landing gear is housed in the external structural fairings that form the outboard sidewalls of the main engine system, as shown in Figure 5. These fairings are structurally integrated with the main shell of the fuselage. These structures provide more than adequate volume to house the retracted main gear and could also be used to house some vehicle or engine systems, if required. Additional structural reinforcement provisions were added to account for strength requirements at the main gear attachments and in the bulkhead at that location.

Graphite/epoxy was chosen as the material system for the baseline integral hydrogen tank because of superior specific properties and its maturity as an airframe structural material system.

This material system has been tested for such concerns as hydrogen containment, cryogenic properties and micro-cracking of the matrix material. Results of this material testing have eliminated these concerns and indicated the material systems are satisfactory for use as a cold integral tank structure.

The tank was designed to operate at 20 psig pressure. The weight of the tank was computed with finite element analysis (Figure 8) to take no advantage of the pressure stabilization of the tanks. The tank design and analysis was provided by the Lockheed Fort Worth Company.

Engine Structure

Description of Structural Design:

The vehicle was set up as a two airbreathing engine design, with each engine consisting of a single set of systems. With the payload bay essentially splitting the mid-body section into two outboard segments, the arrangement of vehicle systems and engine systems into left and right equipment bays naturally drove the design to a two engine arrangement. The engine equipment bays were located immediately over the engine section to the left and right of the payload bay and beneath the mid-body saddle tanks. Vehicle airframe systems bays were located above the saddle tanks and adjacent to the payload bay. Access to all of these equipment bays is easily facilitated through the payload bay without resorting to additional access doors and panels in the exterior surface of the fuselage. This resulted in simpler primary structure and less secondary structure for reinforcement of fuselage penetrations.

The engine structure concept includes structural panels in each repeating flowpath supported by a grid of backing structure, all of which is supported by longitudinal engine/airframe attachment trusses located over each flowpath. The primary structure for supporting the flowpath operating pressure loads is a system of honeycomb panels, backed by integrally attached stiffening beams made up of sine-wave webs and flat caps, as shown in Figure 9. This arrangement transmits the engine pressure, thrust and drag forces into the trusses which are directly attached to the integral tank structure of the airframe. The engine/airframe trusses also serve to carry some airframe loads, because their location, orientation and attachment provide stiffness to the airframe and naturally force some load sharing. This load sharing is not yet optimized. When accomplished, some reduction in tank stiffener weight would be expected, since the airframe integral tank structure was sized for fewer trusses than used in the current arrangement. The unit weights of the engine primary structure were the results of FEM analysis and automated structural design using the structural/thermal sizing code, ST-SIZE (Ref. 5 and 6).

The primary structure is isolated from the hot gas in the flowpath by non-integral heat exchangers that transmit the pressure forces through to the honeycomb panels. The heat exchangers are attached by specially designed fasteners which provide the seal clamping force around the heat exchanger perimeter, but do not restrain the differential thermal growth between primary structure and heat exchanger. The material system chosen for engine primary structure was mostly graphite/epoxy as in the airframe. This is primarily due to its maturity and better specific properties than graphite/polyimide. In the forward portion of the inlet, the primary structure was made of aluminum in order to take advantage of the use of integral aluminum heat exchangers. With an all aluminum structure the heat exchangers may be directly bonded to the honeycomb panel, eliminating the complexity and weight of the fastening and sealing parts. Although the aluminum primary structure is slightly heavier, the net weight is reduced by elimination of the fasteners, seals, insulation and trace cooling parts. The graphite/epoxy material was protected from exceeding a structural re-use temperature limit of 710°R. Because the coefficient of thermal expansion for the graphite/epoxy material is very small, differential thermal growths and stresses will be maintained at small, manageable values.

TPS SIZING/THERMAL MANAGEMENT

Airframe

Thermal Protection System (TPS) Description:

The A/R SSTO baseline vehicle airframe is a cold structure design in which the cryogenic tank bears the structural loads. The ideal TPS system must be weight optimized and designed to survive the temperatures and mechanical loads of flight throughout the trajectory. The optimal TPS to be used depends on the local heat flux, peak surface temperature, length of heat pulse, and aeroacoustic loads. The graphite epoxy tank of the baseline vehicle is thermally protected with a cryogenic, closed cell foam (Rohacell) and a ceramic reusable surface insulation (RSI) material in tile or blanket form (Ref. 1). The leeward (upper) side (shown in Figure 10) of the baseline vehicle uses Tailorable Advanced Blanket Insulation (TABI). The windward (lower) side (shown in Figure 11) of the vehicle uses Fibrous Refractory Composite Insulation (FRCI-12).

The TABI blanket is a woven fabric with triangular cores, which are filled with silica or alumina batting (Ref. 7). The cores add strength against aerodynamic buffeting. The density of the TABI was from 11 to 12 lb/ft3 with a minimum thickness of 0.6 inches and a maximum thickness of 1.3 inches. The maximum temperature capability of TABI is 2760°R. A Protective Ceramic Coating (PCC-B, 0.15 lb/sq ft) is applied to the TABI to provide durability and water proofing. The TABI is an advanced material that has yet to be certified for a specific vehicle.

The FRCI-12 tile is made with silica and aluminoborosilicate fibers; the latter gives the tile more strength and resistance to damage by improving its internal bonding (Ref. 7). The maximum temperature capability of FRCI-12 is 2960°R. The density is 12 lb/ft3. The minimum thickness is 0.2 inches and the maximum thickness is 1.3 inches. The tile has a coating called Toughened Unipiece Fibrous Insulation (TUFI, 60 lb/ft3) to provide durability and water proofing. TUFI coating permeates into the insulation fiber (about 0.10 inches) and was used in preference to reaction-cured borosilicate glass coating (RCG, 104 lb/ft3) which stays on top of the fibers. The TUFI coating can be machined. The FRCI-12 tile is certified and has been flown on the Space Shuttle Orbiter.

TPS Sizing:

An automated one-dimensional transient conduction analysis of the local structure was performed for the leeward and windward sides of the fuselage, using the Systems Improved Numerical Differencing Analyzer program (SINDA, Ref. 8). The internal engine and external afterbody nozzle were not included in the analysis. The automated method performs parametric analyses of plugs to determine insulation thickness and locations where active cooling is needed on the vehicle. A total of 1002 plugs distributed over the surface of the drawn vehicle were generated using PATRAN. Figure 12 shows the nodal distribution of one plug. Aerothermal analysis (as well as aerodynamic) was conducted using APAS (Ref. 9). Vehicle heating rates were obtained at seventeen time points of the ascent and descent trajectory profile. The APAS calculated radiation equilibrium temperature versus time profile was applied to every plug. All 17034 radiation equilibrium temperatures were input into the SINDA transient model. Actively cooled areas were determined, insulation thicknesses were sized, and weights for each plug were totaled for the vehicle.

Boiloff was also calculated along the ascent trajectory for the A/R SSTO vehicle using the SINDA plug model. Heat load and resulting boiloff from the SH2 tanks were totaled for each 60 second interval of the transient analysis. When the liquid and ullage gas were assumed to be in thermal equilibrium at the saturation temperature, boiloff was calculated. Spray bars, a bubble system, and entrainment pumps maintain equilibrium conditions within the SH2 tanks.

Engine

The A/R SSTO vehicle engine cooling concept is a cold structure with mostly nonintegral, actively cooled heat exchangers. Cryogenic hydrogen is used as the fuel and coolant. The objective of the engine heat exchanger design is to minimize the engine's weight, using materials whose thermal and mechanical integrity are maintained throughout the trajectory. The optimal heat exchanger design to be used depends on local heat flux, peak wall temperature, fuel injection temperature and fuel flow rate.

Slush hydrogen is stored in the tank at 20 psig and 25°R. It is pumped to 5500 psi and 60°R before circulating through the cooling panels, then through a turbine to drive the pump, back into the cooling network again, and out into the combustor. The heat exchangers were sized at Mach 15 conditions, where the heat loads are greatest. The cooling panel network was designed to deliver hot hydrogen to the injectors. Detailed thermal and fluid analysis was conducted on the cooling panels to determine the channel dimensions, pressure drop across each panel, and material selection.

Subsystems

The individual subsystems are listed below; the majority of them, however, are highly integrated with each other.

a. Air vehicle thermal control system (AVTCS)
b. Environmental control and life support system (ECLSS)
c. Electrical power generation and conversion system (EPG&C)
d. Hydraulic & actuation
e. Auxiliary power (APU)
f. Reaction control system (RCS)
g. Fuel system
h. Oxidizer system
i. Valves, pressurization, purge & dump (VPP&D)
j. Avionics

The AVTCS will be required to handle both cryogenic and hot hydrogen within the same fluid network. Active thermal cooling is done on the external nozzle, the nose, airframe ramp, engine systems, and the external rocket system. The active cooling panels will deliver hot hydrogen to the engine. Because fuel is used as the coolant, a fail-safe control system is being used. The ECLSS uses standard cryogenic hydrogen control devices, that will be modified for low weight and volume, and provides an operational working environment for the crew. It also provides cooling for the vehicle management system, instrumentation, and the lubrication and hydraulic fluids.

The EPG&C consists of 40 kW 270 VDC fuel cell assemblies. The fuel cells come from existing technology developed for the Space Shuttle program. They use hydrogen and oxygen and provide electrical power primarily for on-orbit duty, but are also used for avionics. APUs provide the hydraulic power for the actuators that control the aero-surfaces and the landing gear. The APU system is derived from an existing Space Shuttle system. The system is driven by a dual mode, gas generator expander cycle turbine using hot hydrogen gas from the fuel system during ascent. This extracted power comes from a hot gas temperature differential which is required to prevent overheating of the material, thereby making the APU power requirements virtually "free" during ascent. The hydraulic system utilizes a conventional hydraulic fluid system that operates at 8000 psia (Ref. 1). Hydraulic fluid cooling heat exchangers dump heat directly into the hydrogen fuel system that provides for the gasification of LH2 and LOX for use in the RCS. The RCS is a previously-developed rocket assembly.

The fuel system is a cryogenic fluid delivery system that supplies LH2 from the vehicle's tanks to the engine turbopumps and actively cooled panels using a series of boost pumps. Because the hydrogen fuel in the tanks was sub-cooled to a slush condition, separate spray and mixing systems in the tanks are required to continually circulate the hydrogen so that it does not stratify; the ullage is kept at the same temperature as the fuel.

The oxidizer system provides LOX to the engine and external rocket system and is composed of both high and low pressure turbopumps. These pumps are used only to supply LOX to the main scramjet engine; the external rocket system has it's own turbomachinery.

The VPP&D is required to provide helium for tank pressurization, vehicle cavity purge and re-pressurization, and pneumatic actuation. Helium is stored at 25°R within the hydrogen fuel tank.

The avionics is based on a proven quad redundant architecture using ADA software and dual fiber optics busses which is intended to provide for autonomous control.

A/R SSTO VEHICLE PERFORMANCE

The mission requirements for the Access to Space Committee study are to deliver a 25000 lb. payload to a hypothetical space station in a 220 nautical mile orbit at an inclination of 51.6 degrees. In addition, 200 ft/s delta-velocity (delta-V) for station docking and maneuver (including 50 ft/s delta-V for RCS), 1% ascent delta-V margin for performance shortfall, and a 5 minute launch window are minimum requirements. A minimum of 1100 nautical mile cross range capability is also required to accommodate a polar mission ascent abort.

Vehicle performance was computed using the POST 3DOF code (Ref. 10). Detailed aerodynamic, propulsion, and pitch plane static trim models were included in all simulations. Takeoff analysis also included aerodynamic and propulsion powered ground effects that account for the influence that the ground has on the inlet and nozzle forces, as well as the effects on body lift and moment. The ascent trajectory profile for the A/R SSTO vehicle is represented in Figure 2.

Performance Results

Axial and normal acceleration levels are shown in Figure 13, where the axial acceleration limit was reached during LOX-augmentation.

The center-of-gravity schedule for the ascent mission is shown in Figure 14. Fortunately, for the A/R SSTO vehicles, there is a significant time-to-double-amplitude margin above the minimum limit. Therefore, there is considerable flexibility in the center-of-gravity schedule needed to maintain a flyable vehicle. As a result, the propellant usage could be scheduled in a way that reduces the trim penalty associated with the vehicle closures reported herein.

Payload delivered to a Space Station orbit (220 nm) and a low-earth orbit (100 NM) as a function of orbital inclination is shown in Figure 15. Payload capability for the airbreathing/rocket SSTO vehicle, at inclinations below 28.5 degrees (due east launch), are significant down to about 17 degrees, whereas a rocket vehicle would have very limited capability. This difference is due to the fact that the airbreathing/rocket SSTO vehicle can generate cross range much more efficiently during the early portion of ascent than a rocket-powered vehicle. The airbreathing/rocket SSTO vehicle has significantly higher effective Isp, especially in the ramjet mode, and also uses aerodynamic lift to steer.

The entry trajectory of the A/R SSTO vehicle was tailored to remain within the temperature capability of the thermal protection system and not to exceed a total acceleration of 1.5 G's. Reentry is performed by flying at low dynamic pressure and nearly constant low angle-of-attack (6°). Banking is used as a control to regulate vertical lift during reentry in order to maintain an acceptable dynamic pressure level/variation. Figure 16 illustrates the Mach number-altitude profile for reentry and includes a time scale on the horizontal axis. Cross range is identified by the tick marks on the curve. This reentry concluded with a nominal cross range of 1850 nm, but the maximum cross range capability is approximately 2500 nm. For this vehicle design, reentry requires active cooling of the engine with liquid hydrogen (LH2) as well as maintaining an engine cavity purge with helium (He) and seals pressurization (He/H2).

Takeoff was performed with full airbreathing and rocket engine thrust at standard sea level conditions. Angle of attack at takeoff was 14 degrees which was near the wing trailing edge clearance limit when accommodating a 20 knot crosswind. The low forebody height to width and length to width ratios facilitated a takeoff velocity of 295 knots and a ground run of 9200 feet.

Potential

The A/R SSTO vehicle can takeoff and climb with any one of its engines out and return to the launch site runway. Each of the two airbreathing engines is contributing 130,000 lbs. of thrust and each of the two rocket engines is contributing 117,000 lbs. of thrust. This takeoff abort scenario was examined with one airbreathing engine shut down at liftoff and is illustrated in Figure 17. The trajectory analysis indicated that the A/R SSTO has no difficulties in gaining altitude, turning, cruising back, and landing on the launch site runway. The vehicle's ground track is plotted in this figure along with the runway and pertinent events.

Mach 12 abort due to the loss of one engine was also examined and is illustrated in Figure 18. Here, the altitude versus Mach number trajectory profile for the aborted ascent mission and return to launch site is shown with significant events identified. Also noted are the distances from the launch site at various points in the trajectory. The trajectory analysis indicates the vehicle can pull-up to lower dynamic pressure, bank and gradually turn, change to ramjet mode during descent, acquire the launch site runway, and land with approximately 20% of the propellant load remaining. Landing with 20% of the propellant load for the above abort mission implies that a Mach 15 abort and return to the launch site runway is highly probable. Aborting at higher Mach numbers would be accomplished by aborting to orbit, where the vehicle would proceed to low elliptic orbit (65 nm apogee) or a once around orbit, then descend and land on the launch site runway.

Flight safety and reliability with this vehicle will be significantly enhanced over today's launch vehicles because the A/R SSTO vehicle is capable of aborting with multiple engines out once an altitude of about 20,000 ft. has been reached. Whether or not abort back to the launch site runway with multiple engines out is possible is yet to be determined; certainly with all engines out, an alternate landing site would have to be found.

The A/R SSTO vehicle has a large launch window, as shown by the solid lines in Figure 19. Both the hypothetical Space Station orbit (51.6° inclination) and the easterly orbit (28.5°) launch windows are shown as a function of ascent delta-V requirement. This large launch window results from the A/R SSTO vehicle requiring a low delta-V to chase the orbit's ascending node due to its high ascent cross range capability, as discussed earlier. Also shown in this figure are corresponding launch window curves for an SSTO rocket vehicle, which are represented by the dashed lines. Note the nearly four-fold advantage of the A/R over the rocket. It should also be noted here that these launch window calculations have not been optimized. Further, the delta-V has a smaller impact on the A/R SSTO vehicle's propellant fraction than for the rocket SSTO vehicle due to the airbreathers high Isp.

The airbreathing/rocket SSTO vehicle has a significant self ferry capability both subsonically and supersonically. The supersonic ferry range is much longer than the subsonic ferry range. This is inherently due to the vehicle being optimized for efficient flight across the entire Mach number range, and that cruise range is proportional to velocity for a given efficiency and propellant fraction. Ferry can be accomplished with either slush or liquid hydrogen.

Having high efficiency at high speeds provides very good hypersonic cruise capability, giving the A/R SSTO vehicle the synergistic capability of rapid long range endo-atmospheric flight, applicable to future high performance and transport aircraft.

The characteristics of the A/R SSTO discussed above offer compelling reasons for the United States to pursue hydrogen-fueled hypersonic airbreathing technology. These compelling reasoning for pursuing viable airbreathing SSTO designs are categorized in Figure 20.

Sensitivities

Imposing a 15% scramjet combustion efficiency reduction on the baseline vehicle from Mach 8 to 15 results in only a 4.2% TOGW penalty. This sensitivity of the A/R SSTO vehicle to scramjet efficiency certainly appears acceptable, but for an accelerating vehicle, thrust is also a primary variable. To determine the sensitivity to thrust, a 5% thrust penalty was applied to the A/R SSTO vehicle from Mach 3 to 15 during the ramjet/scramjet propulsion mode, without impacting the efficiency of the system or the LOX fraction of the vehicle. For mission closure, the TOGW of the A/R SSTO vehicle increased 2.6%. This thrust sensitivity appears acceptable; however, it can be reduced by increasing the LOX fraction of the vehicle at the slight expense of takeoff speed. Therefore, relative to efficiency and thrust of the airbreathing propulsion system, the A/R SSTO vehicle is a robust machine.

Aerodynamic characteristics sensitivities for the A/R SSTO vehicle were performed by imposing constant 5% increases/decreases along the ascent trajectory from Mach 0 to 25. The resultant impact on vehicle TOGW is as follows:

Coefficient perturbation	Delta TOGW, %
+5% CD	+9.6
-5% CD	-8.2
+5% CL	-0.1
-5% CL	+1.1
+5% CM	+0.8
-5% CM	+0.6

Again, these sensitivities appear reasonable and acceptable in a viable aero-space plane; obviously, drag increases are to be avoided as with all aircraft.

The impact on TOGW due to DW growth is shown in Figure 21. The growth in the TOGW as the DW growth increases from 15% to 30% is a modest 30%. The DW growth curve is essentially linear and shows basically no slope increase as the weight growth increases from 15% to 30%.

FUTURE DESIGN TRADES

Aero-space planes, such as the design presented herein, are in their embryonic stage of development and thus have enormous optimization potential, especially when the number and type of variables and systems involved are considered. The A/R SSTO vehicle design team draws on its trade studies and examination of sensitivities to make the following design trade recommendations:

- Tailor the center-of-gravity schedule to reduce trim drag—the time to double amplitude margin will allow such latitude

- Examine converting the twin vertical tails with rudder to rotating twin vertical tails

- Optimize the airbreathing propulsion flowpath
  - shock-on-lip Mach number
  - keel-line
  - contraction ratio
  - combustor length and fuel injector architecture
  - LOX augmentation preburner nozzle exit Mach number

- Optimize systems supporting the airbreathing propulsion flowpath
  - preburner chamber pressure, etc.

- Optimize the structure/tank/TPS
  - consider pressure-stabilization (local buckling failure mode) of the integral Gr/Ep tank
  - consider integral LOX tanks
  - consider TABI on the windward surface

- Optimize the configuration
  - reduce the planform powerlaw
  - utilize the extra volume in engine sidewalls/wheelwells
  - reevaluate engine location

- Examine other configurations
  - wing-bodies with higher fineness ratios and circular

Preliminary assessment indicates that a thorough examination of the above design matrix will reduce the dry weight of the A/R SSTO below 180,000 lbs.

CONCLUDING REMARKS

This A/R SSTO vehicle offers tremendous potential for an orbital vehicle in terms of airplane-like performance characteristics—ground/flight operations flexibility, launch/flight safety and reliability, and larger payload fraction to orbit capability. These are compelling reasons for the United States to pursue viable airbreathing SSTO designs and pertinent technologies. Also, aerospace planes, such as the designs presented herein, are in their embryonic stage of development and thus have enormous optimization potential, especially when the number and type of variables and systems involved are considered.

ACKNOWLEDGEMENTS

1993 Access-to-Space Airbreathing Vehicle Design Team of Langley Research Center's Systems Analysis Office:
Robert Pegg, Dennis Petley, Greg Riebe, and Larren Beacham of NASA LaRC; Paul Moses, John Martin, Craig Collier, Sherri DeShong, Bill Dziedzic, Charles Drummond, Hanee Kabis, Rick Kreis, Peter Pao, Zane Pinckney, Kevin Spoth, and Lawrence Taylor of Lockheed Engineering and Sciences Company; and Laura Bass of Mason and Hanger Services, Inc.

REFERENCES

1. Access to Space Study: Summary Report; Office of Space Systems Development, NASA Headquarters, January 1994.

2. Beckey, I.; Powell, R.; and Austin, R.: NASA Studies Access to Space. Aerospace America, May 1994.

3. Pinckney, S. Z. and Walton, J. T.: Program SRGULL: An Advanced Engineering Model for the Prediction of Airframe-Integrated Subsonic/Supersonic Hydrogen Combustion Ramjet Cycle Performance. NASP TM 1120, January 1991.

4. Sichenhaar, A.; Leonard, J.R.; and Orton, G.F.: Thrust Cell Technology for Modular Engines. Present at 29th Joint Propulsion Conference and Exhibit, AIAA 93-2561, June 1993.

5. Moses, P. L.; Spoth, K. A.; and Collier, C. S.: Structural Analysis and Weight Prediction for Advanced Hypersonic Vehicles. Presented at the ASME Winter Annual Meeting, 1990.

6. Collier, C. S.: Structural Analysis and Sizing of Stiffened, Metal Matrix Composite Panels for Hypersonic Vehicles. AIAA Paper 92-5015, December 1992.

7. Goldstein, H.: Reusable Thermal Protection System Development—A Prospectus. NASA Conference Proceedings CP3157—Current Technology for Thermal Protection Systems, pp. 1-19, February 1992.

8. Petley, D. H.; Jones, S. C.; and Dziedzic, W. M.: Integrated Numerical Methods for Hypersonic Aircraft Cooling Systems Analysis. Presented at the 30th Aerospace Sciences Meeting and Exhibit, AIAA Paper 92-0254, January 1992.

9. Cruz, C. I. and Wilhite, A. W.: Prediction of High-Speed Aerodynamic Characteristics Using the Aerodynamic Preliminary Analysis System (APAS), AIAA-89-2173, July 1989.

10. Braur, G. L.; Cornick, D. E.; and Stevenson, R.: Capabilities and Applications of the Program to Optimize Simulated Trajectories. NASA CR-2770, February 1977.

- 25,000 lb. payload
- 51.6° declination / 220 nm. orbit

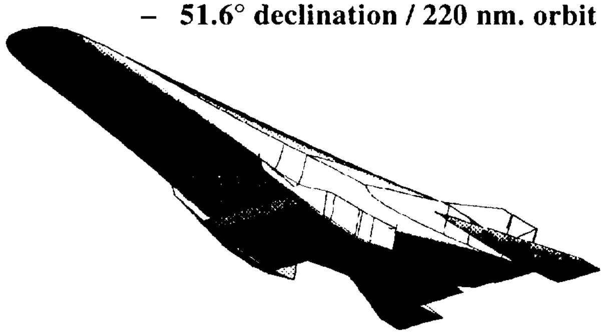

Figure 1. Airbreathing/Rocket (A/R) Single-Stage-to-Orbit (SSTO) Vehicle (referenced from Access-to-Space study)

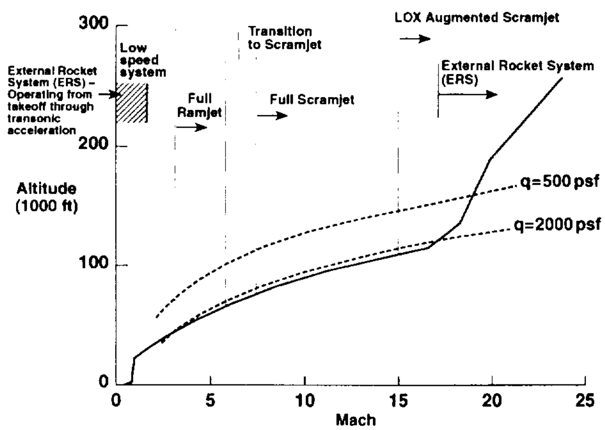

Figure 2. Representative ascent trajectory

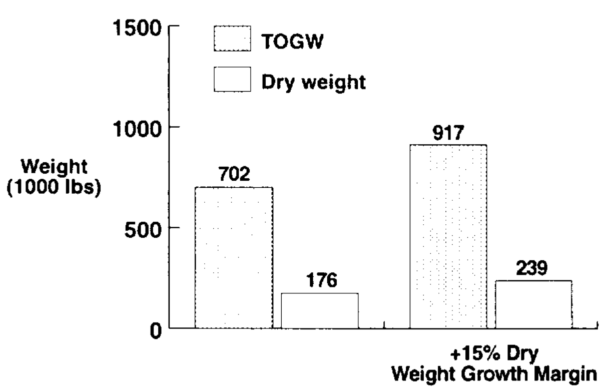

Figure 3. Baseline vehicle closure weights—graphite/epoxy integral tank structure with Rohacell insulation (FRCI-12 TPS on windward surfaces and TABI TPS on upper surface)

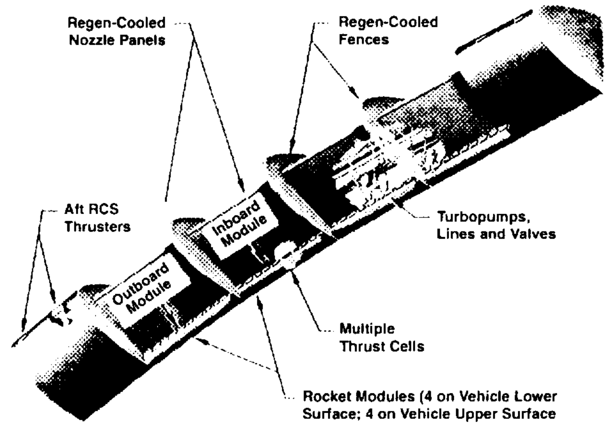

Figure 4. General arrangement of low drag, integrated rocket system

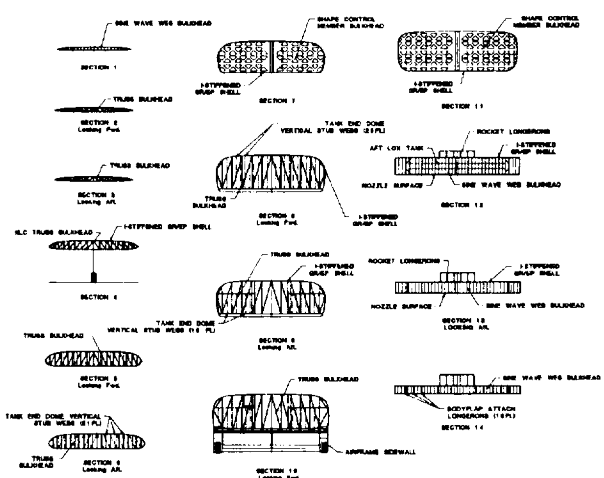

Figure 5. A/R SSTO vehicle structural cross-sections

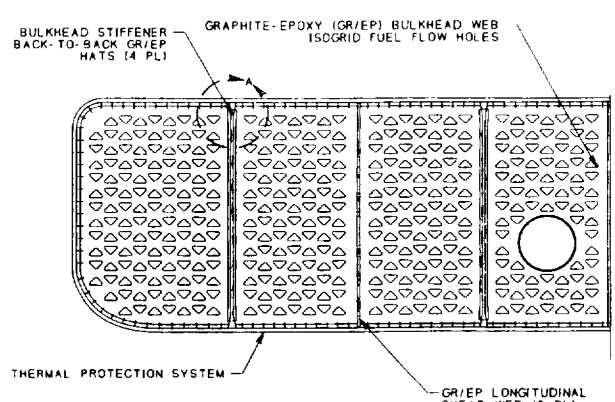

Figure 6. Vehicle shape control member

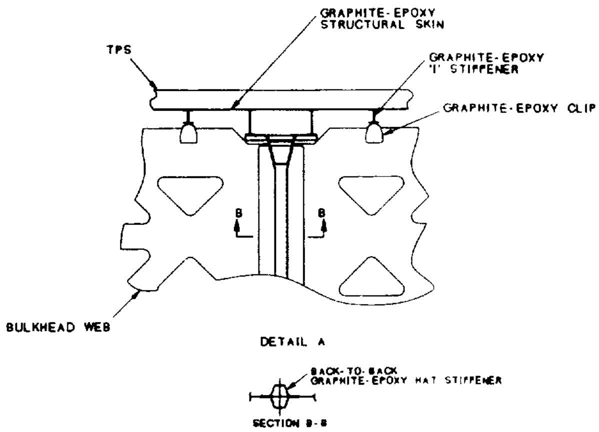

Figure 7. Detail of vehicle shape control member

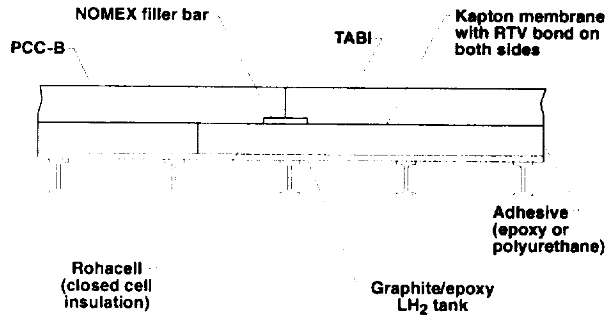

Figure 10. Cold integral baseline structure (upper airframe surface, graphite/epoxy with TABI/Rohacell TPS)

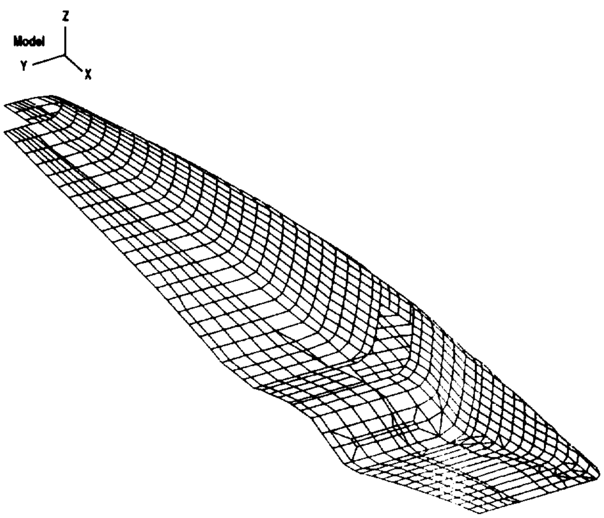

Figure 8. Baseline vehicle primary structure finite element model (FEM, surrogate), bottom view

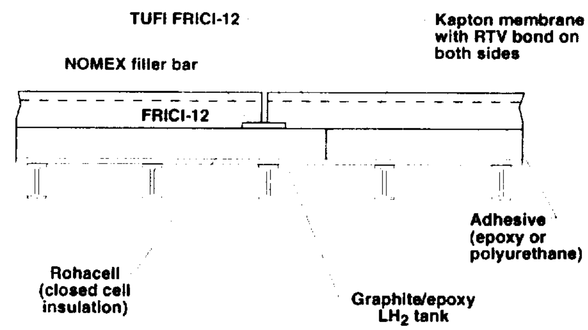

Figure 11. Cold integral baseline structure (lower airframe surface, graphite/epoxy with FRICI-12/Rohacell TPS)

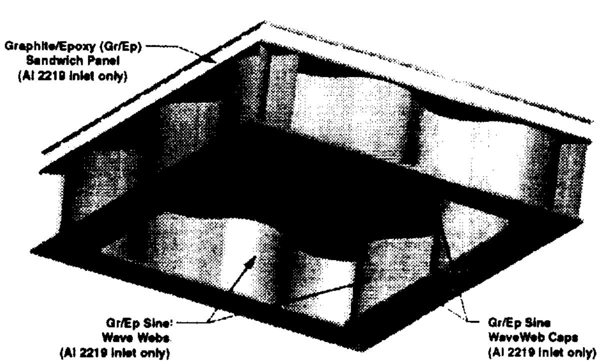

Figure 9. Engine primary structure concept

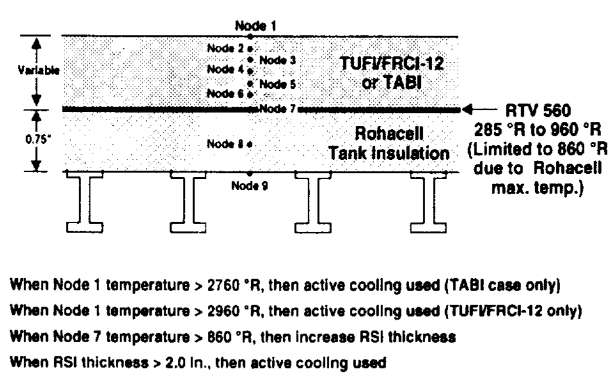

Figure 12. A/R SSTO vehicle 1-D thermal analysis plug model (1002 plugs, ascent and descent analyzed)

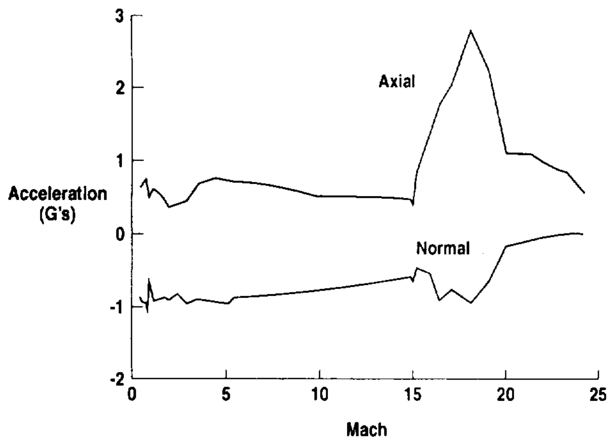

Figure 13. Normal and axial acceleration

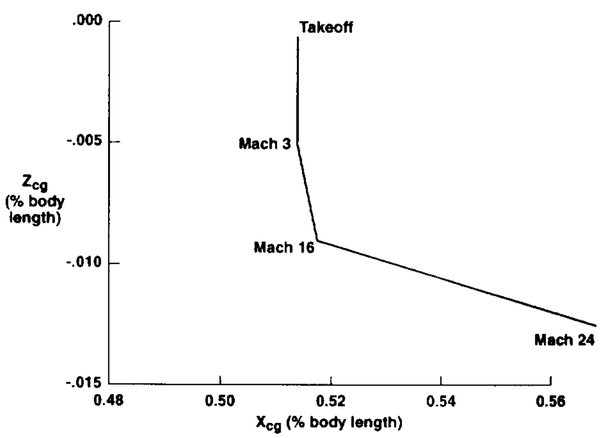

Figure 14. Center of gravity schedule for ascent

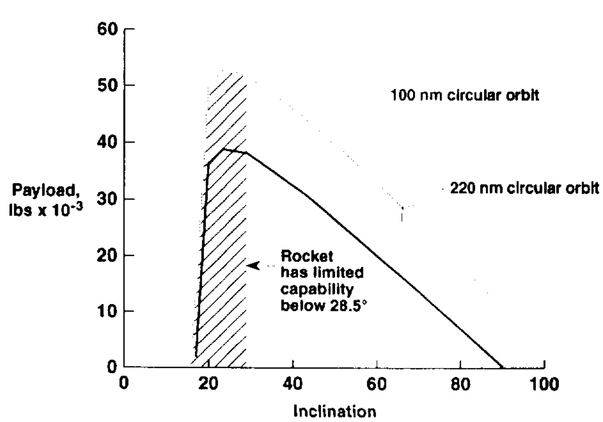

Figure 15. Payload delivered to orbit from KSC as a function of orbital inclination

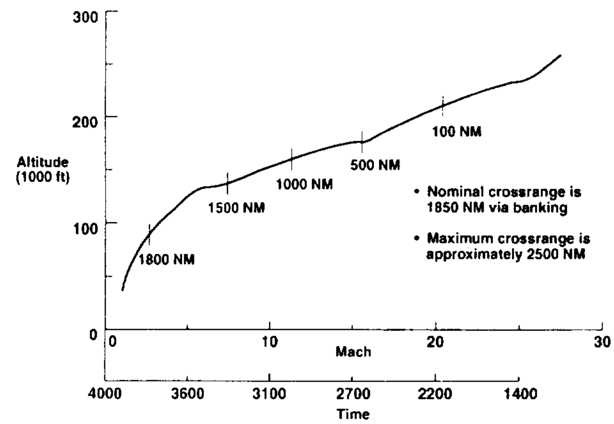

Figure 16. A/R SSTO vehicle descent trajectory

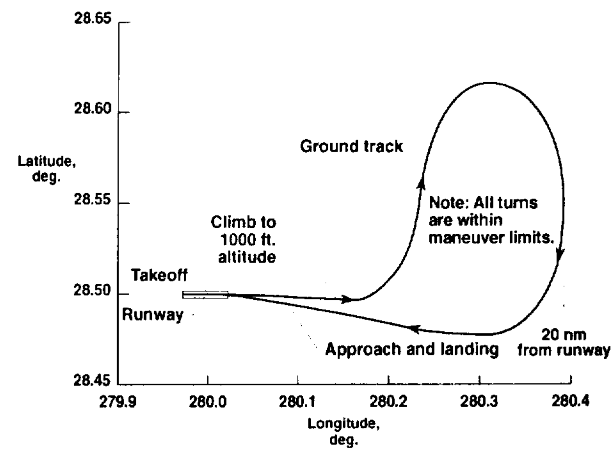

Figure 17. Takeoff abort scenario

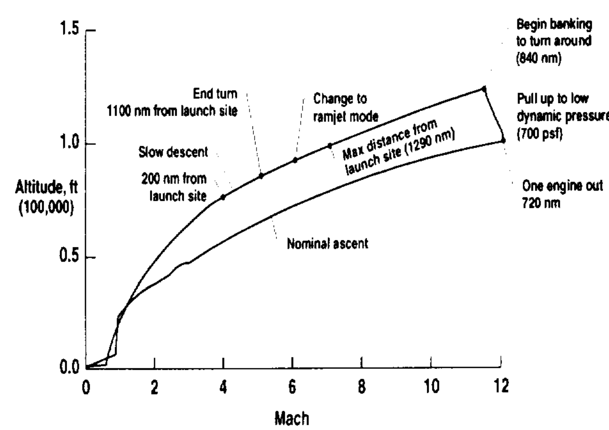

Figure 18. Mach 12 ascent abort scenario to launch site runway

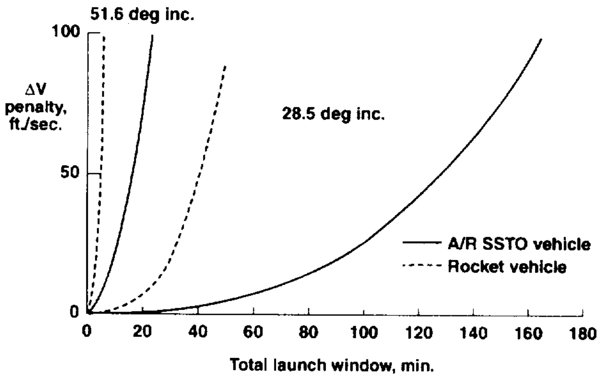

Figure 19. Launch window ΔV penalty, 220 nmi orbit, 51.6° inclination

Performance
- Large potential in terms of payload weight, range/orbit, and delivery times
- Endoatmospheric operations/hypersonic cruise and space access with same vehicle
- Subsonic and/or supersonic self ferry capability

Mission Flexibility
- Large launch window potential
- Launch offset capability
- Orbital plane change through endoatmosphere lifting/powered maneuvers
- Large cross range capability

Risk Reduction
- Gradual step and check engine start-up and shutdown
- Horizontal takeoff/abort capability
- Endoatmospheric abort during ascent with powered flyback

Environmental
- Relatively low noise levels
- Water vapor exhaust

Operations
- Conventional aircraft operations and logistics (horizontal takeoff/horizontal landing)
- Quick turn-around times

Figure 20. Compelling reasons for airbreathing SSTO

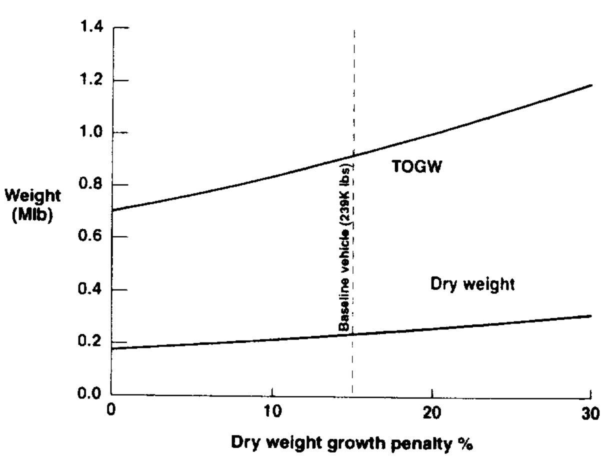

Figure 21. Weight growth sensitivity